reflection coefficient can then be calculated using the results of these expressions. These results can be extended to broadband microwave amplifier design by finding the optimum source reflection coefficient over a range of frequencies. The inclusion of these expressions in the advanced computer aided design tools that are now available would significantly simplify the low noise microwave amplifier design process.

REFERENCES

[1] G. D. Vendelin, A. M. Pavio, and U. L. Rohde, *Microwave Circuit Design Using Linear and Nonlinear Techniques.* New York: Wiley, 1990, pp. 84–93.

[2] G. Gonzalez, *Microwave Transistor Amplifiers: Analysis and Design.* Englewood Cliffs, NJ: Prentice-Hall, 1984, pp. 91–125.

[3] L. Besser, "Stability considerations of low-noise transistor amplifiers with simultaneous noise and power match," in *IEEE MTT-S Int. Microwave Symp. Dig.,* 1975, pp. 327–329.

[4] S. Iverson, "The effect of feedback on noise figure," *Proc. IEEE,* vol. 63, pp. 540–542, Mar. 1975.

[5] G. D. Vendelin, "Feedback effects on the noise performance of GaAs Mesfets," in *IEEE MTT-S Int. Microwave Symp. Dig.,* 1975, pp. 324–326.

[6] W. A. Suter, "Feedback and parasitic effects on noise," *Microwave J.,* pp. 123–129, Feb. 1983.

[7] H. Fukui, "Available power gain, noise figure, and noise measure of two-ports and their graphical representation," *IEEE Trans. Circuit Theory,* vol. CT-13, pp. 137–142, June 1966.

[8] C. R. Poole and D. K. Paul, "Optimum noise measure terminations for microwave transistor amplifiers," *IEEE Trans. Microwave Theory Tech.,* vol. MTT-33, no. 11, pp. 1254–1257, Nov. 1985.

[9] G. Gonzalez, *Microwave Transistor Amplifiers: Analysis and Design.* Englewood Cliffs, NJ: Prentice-Hall, 1984, pp. 92 and 123.

Simple and Explicit Formulas for the Design and Analysis of Asymmetrical V-Shaped Microshield Line

Kwok-Keung M. Cheng and Ian D. Robertson

Abstract— **This paper presents some simple, explicit and practical formulas for the evaluation of the quasi-TEM characteristic parameters of asymmetrical V-shaped microshield line, based on a conformal mapping procedure. These formulas give very accurate results in terms of elementary functions rather than the exact solution in terms of difficult functions. Two sets of expressions are described using first and second order approximations. These equations are easy to implement, thus making it an excellent choice for use in computer aided design, analysis and optimization of V-shaped microshield structures.**

I. INTRODUCTION

Recently, the microshield line, a new type of transmission line [1]–[4], has been the subject of growing interest as it has presented a solution to technical and technological problems encountered in the design of microstrip and coplanar lines. The microshield line, when compared with the conventional ones, has the ability to operate without the need for via-holes or the use of air-bridges for ground equalization. There are further advantages like reduced radiation loss, reduced electromagnetic coupling between adjacent lines, and the availability of a wide range of impedances. Various types of microshield structures have been reported [1], [2], and [4] including the rectangular, V, elliptic, and circular-shaped transmission lines. The quasi-TEM study of V-shaped microshield line (VSML) has been performed both by a method of moments [3] and a conformal mapping technique [4]. These methods give highly accurate results but are computationally intensive.

In this paper, a set of CAD-orientated closed form expressions that can be readily evaluated is derived for the characterisation of asymmetrical VSML. Both a first and a second order model for the approximation of the exact solution are presented. The analyses are based on the conformal mapping method and the assumptions of pure-TEM propagation and no dispersion effect. The characterization of the asymmetrical version of the VSML is extremely important because it could offer additional flexibility in the design of integrated circuits. Futhermore, it also allows one to evaluate the actual characteristics of a VSML normally designed to be symmetrical, but the fabrication of which is imperfect.

II. ANALYSIS OF ASYMMETRICAL VSML

This section gives a brief derivation of the characteristic parameters of an asymmetrical V-shaped microshield line. Similar mapping procedure has been described in [4] for a symmetrical line structure. The asymmetrical VSML configuration to be analyzed is shown in Fig. 1(a), where the ground plane is bent within the dielectric in a V-shape to form the equal sides of an isosceles triangle. All metallic conductors are assumed to be infinitely thin and perfectly conducting, and the ground planes to be sufficiently wide as to be considered infinite in the model. It is assumed that the air-dielectric boundary between the center conductor and the upper ground plane behaves like a perfect magnetic wall. This ensures that no electric field lines emanating into the air from the center conductor cross the air-dielectric boundary. Although this assumption is hardly verified for large slots, it has proven to yield excellent results for practical line dimensions. The center conductor, of width b, is placed between the two ground planes, which are located on a substrate of relative permittivity ε_r. The overall capacitance per unit length of the line can therefore be considered as the sum of the capacitance of the upper region (air) and the lower region (dielectric). The capacitance of the lower region can be evaluated through a suitable sequence of conformal mappings. First, the interior of the V-shaped region is mapped onto the t domain (Fig. 1) by the Schwartz-Christoffel transformation

$$z = A\int_0^t (t^2-1)^{(-2\beta+\pi)/2\pi}dt \tag{1}$$

and then back onto the w domain using a second mapping function

$$w = \int_0^t \frac{dt}{\sqrt{(t+t_E)(t-t_E)(t-t_C)(t-t_D)}} \tag{2}$$

where 2β is the flare angle (in radian) of the V-shaped wall. The intermediate parameters t_C, t_D and t_E, are evaluated by the following implicit expressions, as a function of β and the geometrical ratios, $d_1/b, d_2/b$ and b/W, of the structure

$$\frac{z_E}{z_B} = \frac{d_2+d_1+b}{W} = \frac{\zeta(\arcsin(t_E))}{\zeta(\pi/2)} \tag{3a}$$

Manuscript received November 29, 1994; revised June 29, 1995. This work was supported by The Engineering and Physical Sciences Research Council (EPSRC), UK.

The authors are with the Communication Research Group, Department of Electronic & Electrical Engineering, King's College London, University of London, Strand, London, England WC2R 2LS.

IEEE Log Number 9414243.

$$\frac{z_C}{z_B} = \frac{d_2 - d_1 - b}{W'} = \frac{\zeta(\arcsin(t_C))}{\zeta(\pi/2)} \tag{3b}$$

$$\frac{z_D}{z_B} = \frac{d_2 - d_1 + b}{W'} = \frac{\zeta(\arcsin(t_D))}{\zeta(\pi/2)} \tag{3c}$$

$$\zeta(\phi) = \int_0^{\phi} (\cos\theta)^{-2\beta/\pi} d\theta. \tag{3d}$$

If the capacitances of the upper and lower regions are referred to as C_1 and C_2, respectively, then the overall capacitance per unit length of the line is given as [6]

$$C_T(\varepsilon_r) = C_1 + C_2 = \varepsilon_0 \frac{K(k_1)}{K'(k_1)} + \varepsilon_r \varepsilon_0 \frac{K(k_2)}{K'(k_2)} \tag{4}$$

where

$$k_1 = \sqrt{\frac{b(b + d_1 + d_2)}{(b + d_1)(b + d_2)}}$$

$$k_2 = \sqrt{\frac{2t_E(t_D - t_C)}{(t_E + t_D)(t_E - t_C)}}.$$

$K(k)$ is the complete elliptic integral of the first kind. Hence, the effective permittivity and the characteristic impedance of the line are [6], respectively

$$\varepsilon_{\text{eff}} = \frac{C_T(\varepsilon_r)}{C_T(1)} = 1 + q(\varepsilon_r - 1) \tag{5}$$

where the filling factor, q, is expressed as

$$q = \frac{K(k_2)/K'(k_2)}{K(k_1)/K'(k_1) + K(k_2)/K'(k_2)}$$

and

$$Z_0 = \frac{120\pi}{\sqrt{\varepsilon_{\text{eff}}}} \frac{1}{K(k_1)/K'(k_1) + K(k_2)/K'(k_2)}. \tag{6}$$

The line parameters can therefore be calculated from (5) and (6) using the simple formulas of Hilberg [5] for the ratio $K(k)/K'(k)$. The main drawback of the present solution is that no simple and explicit expressions is available for the parameters t_C, t_D, and t_E in terms of β and the geometrical ratios. Iterative numerical methods [7] are therefore required to obtain the solution which leads to long computation time. In the following sections, a set of simple and explicit analytical solutions will be described.

III. First-Order Model

In order to develop a simple expression for the integral in (3d), the range of integration is first split into two segments with the dividing point at $\phi = \frac{\pi}{2} - 1$, as in Fig. 2. The original integrand is then approximated by simple functions in which closed-form expressions are readily available. Mathematically, the two functions can be chosen as

$$\left(\frac{1}{\cos\phi}\right)^{2\beta/\pi} \approx 1 \qquad \text{for } 0 \le \phi \le \frac{\pi}{2} - 1 \tag{7a}$$

and

$$\left(\frac{1}{\cos\phi}\right)^{2\beta/\pi} \approx \left(\frac{1}{\pi/2 - \phi}\right)^{2\beta/\pi} \qquad \text{for } \frac{\pi}{2} - 1 \le \phi \le \frac{\pi}{2}. \tag{7b}$$

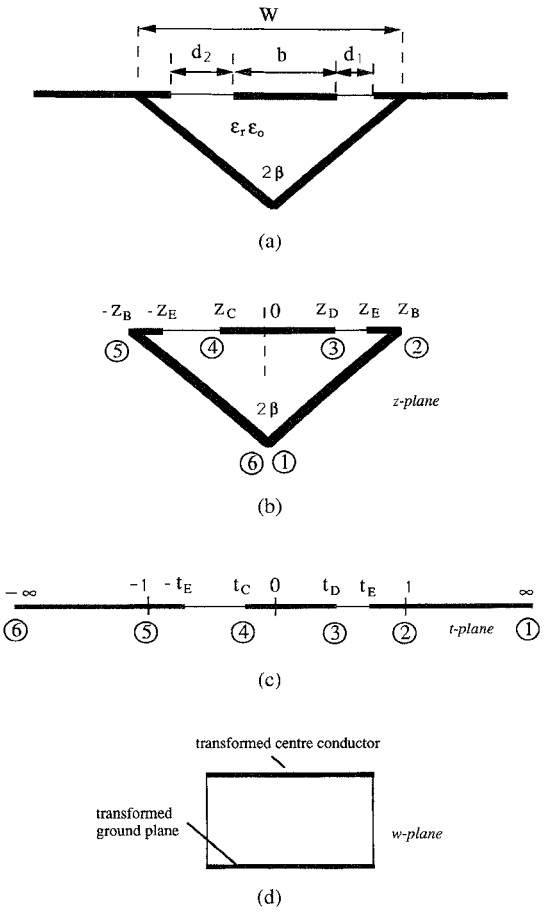

Fig. 1. Conformal mapping of asymmetrical VSML.

Using these approximating functions, the area under the new curve can therefore be expressed as

$$\zeta(\phi) = \phi \qquad \text{for } 0 \le \phi \le \frac{\pi}{2} - 1 \tag{8a}$$

$$\zeta(\phi) = \alpha - \frac{\left(\frac{\pi}{2} - \phi\right)^{1 - 2\beta/\pi}}{1 - 2\beta/\pi} \qquad \text{for } \frac{\pi}{2} - 1 \le \phi \le \frac{\pi}{2} \tag{8b}$$

where

$$\alpha = \frac{\pi}{2} - 1 + \frac{1}{1 - 2\beta/\pi}. \tag{8c}$$

Substituting (8) into (3), and after some manipulations, the following formulas are then obtained

$$t = \sin\left(\alpha \frac{z}{z_B}\right) \qquad \text{for } 0 \le \frac{z}{z_B} \le \frac{\pi/2 - 1}{\alpha} \tag{9a}$$

$$t = \cos\left\{\left[\alpha\left(1 - \frac{2\beta}{\pi}\right)\left(1 - \frac{z}{z_B}\right)\right]^{\frac{1}{1 - 2\beta/\pi}}\right\} \qquad \text{for } \frac{\pi/2 - 1}{\alpha} \le \frac{z}{z_B} \le 1. \tag{9b}$$

IV. Second-Order Model

This model (Fig. 3) is very similar to the previous one, except that the central region of the curve is approximated by a third function

$$\left(\frac{1}{\cos\phi}\right)^{2\beta/\pi} \approx \left(\frac{\sqrt{2}}{1 - \phi + \pi/4}\right)^{2\beta/\pi} \qquad \text{for } 1 + \frac{\pi}{4} - \sqrt{2} \le \phi \le \frac{\pi}{4} + \frac{\frac{\pi}{2\sqrt{2}} - 1}{\sqrt{2} - 1}. \tag{10}$$

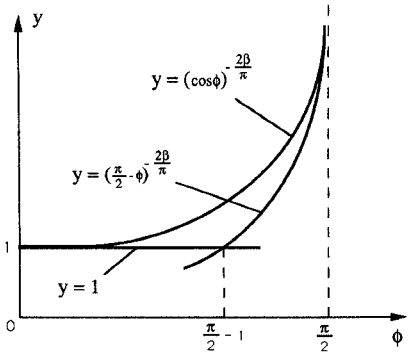

Fig. 2. first order model.

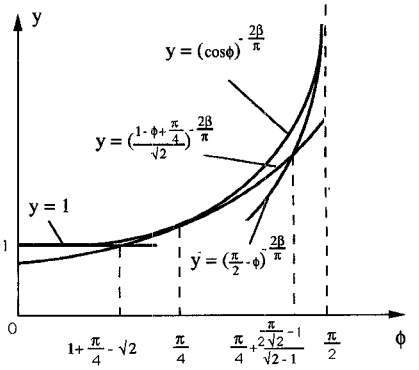

Fig. 3. second order model.

Hence, the new expressions for the area under this curve is given by

$$\zeta(\phi) = \phi \qquad \text{for } 0 \le \phi \le 1 + \frac{\pi}{4} - \sqrt{2} \tag{11a}$$

$$\zeta(\phi) = 1 + \frac{\pi}{4} - \sqrt{2} + \frac{\sqrt{2}}{1 - 2\beta/\pi} \times \left[1 - \left(\frac{1 + \frac{\pi}{4} - \phi}{\sqrt{2}}\right)^{1-2\beta/\pi}\right]$$

$$\text{for } 1 + \frac{\pi}{2} - \sqrt{2} \le \phi \le \frac{\pi}{4} + \frac{\frac{\pi}{2\sqrt{2}} - 1}{\sqrt{2} - 1} \tag{11b}$$

$$\zeta(\phi) = \gamma - \frac{\left(\frac{\pi}{2} - \phi\right)^{1-2\beta/\pi}}{1 - 2\beta/\pi}$$

$$\text{for } \frac{\pi}{4} + \frac{\frac{\pi}{2\sqrt{2}} - 1}{\sqrt{2} - 1} \le \phi \le \frac{\pi}{2} \tag{11c}$$

where

$$\gamma = 1 + \frac{\pi}{4} - \sqrt{2} + \frac{\sqrt{2}}{1 - 2\beta/\pi} \times \left[1 - \left(1 - \frac{1}{\sqrt{2}}\right)\left(\frac{1 - \frac{\pi}{4}}{\sqrt{2} - 1}\right)^{1-2\beta/\pi}\right]. \tag{11d}$$

Combining (3) and (11), the new set of design formulas is therefore given by

$$t = \sin\left(\gamma \frac{z}{z_B}\right) \qquad \text{for } 0 \le \frac{z}{z_B} \le \frac{1 + \pi/4 - \sqrt{2}}{\gamma} \tag{12a}$$

$$t = \sin\left\{1 + \frac{\pi}{4} - \sqrt{2}\left[1 - \frac{1 - 2\beta/\pi}{\sqrt{2}} \times \left(\gamma \frac{z}{z_B} - 1 - \frac{\pi}{4} + \sqrt{2}\right)\right]^{\frac{1}{1-2\beta/\pi}}\right\}$$

$$\text{for } \frac{1 + \pi/4 - \sqrt{2}}{\gamma} \le \frac{z}{z_B} \le 1 - \frac{1}{\gamma(1 - 2\beta/\pi)}\left(\frac{1 - \pi/4}{\sqrt{2} - 1}\right)^{1-2\beta/\pi} \tag{12b}$$

$$t = \cos\left\{\left[\gamma\left(1 - \frac{2\beta}{\pi}\right)\left(1 - \frac{z}{z_B}\right)\right]^{\frac{1}{1-2\beta/\pi}}\right\}$$

$$\text{for } 1 - \frac{1}{\gamma(1 - 2\beta/\pi)}\left(\frac{1 - \pi/4}{\sqrt{2} - 1}\right)^{1-2\beta/\pi} \le \frac{z}{z_B} \le 1. \tag{12c}$$

TABLE I
CALCULATED CHARACTERISTIC IMPEDANCE (IN OHM) OF VSML WITH B = 30°, $d_1 = d_2, W = b + 2d_1$

b / (b + d1 + d2)	Numerical method	1st order model	2nd order model
0.1	144.0	144.4	144.1
0.2	112.1	112.3	112.0
0.3	93.1	92.8	92.9
0.4	79.2	78.8	79.1
0.5	68.0	67.6	68.0
0.6	58.4	58.0	58.3
0.7	49.7	49.4	49.6
0.8	41.2	40.9	41.1
0.9	32.0	31.8	31.9

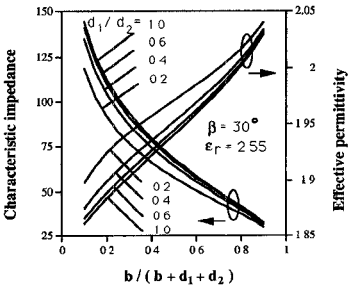

Fig. 4. Variation of Z_0 and ε_{eff} as a function of shape ratio taking d_1/d_2 as a parameter for VSML, $W = b + d_1 + d_2, \beta = 30°$.

It can be seen from expressions (10) and (12) that the value of t is now given explicitly in terms of elementary functions of geometrical parameters β and $\frac{z}{z_B}$.

V. DISCUSSIONS

We have described three methods, the numerical solution and two sets of formulas, for obtaining the characteristic impedances of VSML. In order to validate the accuracy of these expressions, results obtained by the three approaches are tabulated in Table I for comparison. Note that by just using the first order model, the set of formulas derived is sufficiently accurate for many practical applications. The second order model gives impedance calculations of better than 0.2% inaccuracy.

Examples of design curves of asymmetrical VSML are given in Figs. 4 and 5, for different values of β. From these graphs, it can be concluded that, for a given shape ratio $b/(b + d_1 + d_2)$, the line asymmetry leads to a decrease of its characteristic impedance and to

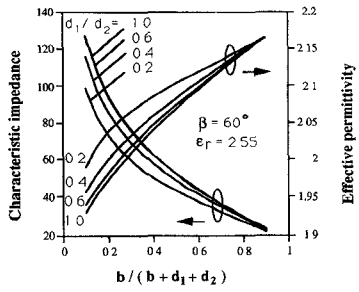

Fig. 5. Variation of Z_0 and ε_{eff} as a function of shape ratio taking d_1/d_2 as a parameter for VSML, $W = b + d_1 + d_2, \beta = 60°$.

an increase of its relative effective dielectric constant. However, these variations are not significant for small asymmetry and large shape ratio. For a given shape ratio and asymmetrical factor (d_1/d_2), the impedance is higher with lower value of β. This is simply because of the decreasing separation between the center conductor and the ground plane. Note that due to the many available parameters in design, a wide range of impedances may therefore be obtained.

VI. Conclusion

Two sets of simple, explicit formulas have been developed for the evaluation of the quasi-TEM characteristic parameters of asymmetrical V-shaped microshield line. The numerical accuracy of these expressions is verified by comparing the results with the ones obtained by a standard numerical technique. It has been observed that the accuracy of the new set of formulas are good enough in many practical situations. Higher accuracy may further be achieved, in a step by step manner, by increasing the order of the model in representating the original integral. The numerical results show that the characteristic impedance and relative effective permittivity of VSML vary slowly with the onset of asymmetry.

References

[1] N. I. Dib, W. P. Harokopus Jr., L. P. B. Katehi, C. C. Ling, and G. M. Rebeiz, "Study of a novel planar transmission line," in *1991 IEEE MIT-S Int. Microwave Symp. Dig.*, pp. 623–626.

[2] N. I. Dib and L. P. B. Katehi, "Impedance calculation for the microshield line," *IEEE Microwave and Guided Wave Lett.*, vol. 2, pp. 406–408, Oct. 1992.

[3] J. E. Schutt-Aine, "Static analysis of V transmission lines," *IEEE Trans. Microwave Theory Tech.*, vol. 40, pp. 659–664, Apr. 1992.

[4] N. Yuan, C. Ruan and W. Lin, "Analytical analyses of V, elliptic, and circular-shaped microshield transmission lines," *IEEE Trans. Microwave Theory Tech.*, vol. MTT-42, pp. 855–858, May 1994.

[5] W. Hilberg, "From approximations to exact relations for characteristic impedances," *IEEE Trans. Microwave Theory Tech.*, vol. MTT-17, pp. 259–265, May 1969.

[6] G. Ghione and C. Naldi, "Coplanar waveguides for MMIC applications: effect of upper shielding, conductor backing, finite-extent ground planes, and line-to-line coupling," *IEEE Trans. Microwave Theory Tech.*, vol. MTT-35, pp. 260–267, Mar. 1987.

[7] W. Press, B. Flannery, S. Teukolsky, and W. Vetterling, *Numerical Recipes, The Art of Scientific Computing*. Cambridge, England: Cambridge Univ. Press, 1986.

Nonlinear Yield Analysis and Optimization of Monolithic Microwave Integrated Circuits

Stefano D'Agostino and Claudio Paoloni

***Abstract*—In this paper, a discussion about nonlinear yield evaluation and nonlinear yield optimization of MMIC circuits using a physics-based nonlinear lumped-element MESFET model is presented. The lumped elements of the MESFET model are directly calculated by closed expressions related to process parameters. One of the main features of the model is the easy and effective implementation in commercial CAD tools. It allows the use of nonlinear yield algorithms assuming, as statistical variables, the parameters of the technological process, such as: doping density, gate channel length, etc., maintaining at the same time, the advantages of lumped-element MESFET model, in particular fast computation and reduction of convergence problems in harmonic balance for complex circuit topologies.**

I. Introduction

MMIC technology, due to the extremely limited postprocessing tuning facility, requires an accurate prediction of the manufacturing yield of circuit and an effective procedure to improve the yield if not adequate. Many contributions regard yield analysis as well as yield optimization were presented in literature [1]–[6].

Typically a MMIC circuit is composed by active and passive components on the same substrate. Both components contribute to circuit yield. Passive elements are mainly sensible to geometrical variations and to the substrate parameters as effective dielectric constant ϵ_r and height h, while the active elements are also sensible to process variations.

To effectively evaluate the yield of the circuit, and eventually improve it, the use of models of circuit elements accurately related to the MMIC process parameters, to account for variations of the electrical behavior caused by the variations in the process parameters is mandatory. Especially if technological process is well established and allows high performance circuits, an accurate yield evaluation and yield optimization bring forth relevant advantages by finely controlling the process parameters around their nominal values.

Two approaches for yield analysis, from the circuit point of view, can be distinguished. The first one is based on the use of lumped-element model of active devices for both small signal and large signal cases. The yield analysis is performed varying statistically the values of the linear and nonlinear lumped elements composing the model such as capacitors, inductors, resistors, and nonlinear components. The advantage of this approach consists in the immediate implementation of the active device model in commercial CAD tools that usually contain Monte Carlo analysis algorithms. The computational time to obtain the final result is very short. The drawback of the approach consists in the lack of any direct relationship with process parameters and even if the result of yield analysis can be indicative, a following yield optimization is hardly applicable to the technological process.

The second approach is based on circuit models of active devices related to process parameters. The yield analysis performed by this approach is very accurate and is directly linked to the parameters of

Manuscript received January 12, 1995; revised June 29, 1995.

S. D'Agostino is with the University of Roma La Sapienza, Department of Electronic Engineering, 00184, Rome, Italy.

C. Paoloni is with the University of Roma Tor Vergata, Department of Electrical Engineering, 00133, Rome, Italy.

IEEE Log Number 9414316.